In vitro characterization of fluorescence by unbound excitation from luminescence: Broadening the scope of energy transfer

Alexandra Holland, Florian Rückerl, Joseph Dragavon, Abdessalem Rekiki, Jean-Yves Tinevez, Régis R. Tournebize, Spencer Shorte

▶ **To cite this version:**

Alexandra Holland, Florian Rückerl, Joseph Dragavon, Abdessalem Rekiki, Jean-Yves Tinevez, et al.. In vitro characterization of fluorescence by unbound excitation from luminescence: Broadening the scope of energy transfer. Methods, 2014, 66 (2), pp.353-361. 10.1016/j.ymeth.2013.09.005 . pasteur-02616460

HAL Id: pasteur-02616460
https://pasteur.hal.science/pasteur-02616460

Submitted on 24 May 2020

HAL is a multi-disciplinary open access archive for the deposit and dissemination of scientific research documents, whether they are published or not. The documents may come from teaching and research institutions in France or abroad, or from public or private research centers.

L'archive ouverte pluridisciplinaire **HAL**, est destinée au dépôt et à la diffusion de documents scientifiques de niveau recherche, publiés ou non, émanant des établissements d'enseignement et de recherche français ou étrangers, des laboratoires publics ou privés.

Distributed under a Creative Commons Attribution - NonCommercial - ShareAlike 4.0 International License

Methods 66 (2014) 353–361

Contents lists available at ScienceDirect

Methods

journal homepage: www.elsevier.com/locate/ymeth

In vitro characterization of fluorescence by unbound excitation from luminescence: Broadening the scope of energy transfer

Alexandra D. Holland [a], Florian Rückerl [a], Joseph M. Dragavon [a], Abdessalem Rekiki [a], Jean-Yves Tinevez [a], Régis Tournebize [a,b,*], Spencer L. Shorte [a,*]

[a] Plate-Forme d'Imagerie Dynamique, Imagopole, Institut Pasteur, 25-28 Rue du Dr. Roux, 75724 Paris cedex 15, France
[b] Unité INSERM U786, Institut Pasteur, 28 rue du Dr Roux, 75724 Paris cedex 15, France

ARTICLE INFO

Article history:
Available online 14 September 2013

Keywords:
BRET
CRET
FRET
FUEL

ABSTRACT

Energy transfer mechanisms represent the basis for an array of valuable tools to infer interactions *in vitro* and *in vivo*, enhance detection or resolve interspecies distances such as with resonance. Based upon our own previously published studies and new results shown here we present a novel framework describing for the first time a model giving a view of the biophysical relationship between Fluorescence by Unbound Excitation from Luminescence (FUEL), a conventional radiative excitation–emission process, and bioluminescence resonance energy transfer. We show here that in homogeneous solutions and in fluorophore-targeted bacteria, FUEL is the dominant mechanism responsible for the production of red-shifted photons. The minor resonance contribution was ascertained by comparing the intensity of the experimental signal to its theoretical resonance counterpart. Distinctive features of the *in vitro* FUEL signal include a macroscopic depth dependency, a lack of enhancement upon targeting at a constant fluorophore concentration c_f and a non-square dependency on c_f. Significantly, FUEL is an important, so far overlooked, component of all resonance phenomena which should guide the design of appropriate controls when elucidating interactions. Last, our results highlight the potential for FUEL as a means to enhance *in vivo* and *in vitro* detection through complex media while alleviating the need for targeting.

© 2013 The Authors. Published by Elsevier Inc. Open access under CC BY-NC-SA license.

1. Introduction

The recent emergence of greatly improved single photon detectors has resulted in major advances in the use of luminescence for deep-tissue analysis in living, intact organisms. Such *state-of-the-art* applications offer robust mainstay technology which has become a routine part of *in vivo* pre-clinical studies in diverse disciplines from development, to cancer, immunology, and infection [1–6]. However, the trend towards *in vivo* optical imaging has highlighted new challenges, notably regarding the use of genetically encoded luminescent probes. Indeed, most natural bioluminescent molecules available as probes for such studies characteristically emit a blue-green light that is strongly absorbed by biological tissues. Consequently, the main strategy to enhance luminescent probes detection has entailed shifting photonic emission towards the longer red wavelengths, which are absorbed much less in mammalian tissue. Such optimization has so far been achieved using either direct genetic manipulation, and/or resonance energy transfer methods.

In contrast to the success of either red-shifting fluorescent chemicals [7] or genetically engineering fluorescent probes [8–10], there has been rather less progress towards the same with chemiluminescent and bioluminescent probes. For example, mutagenesis of the luciferase from the *Renilla reniformis* coelenterate has achieved only modest red emission shifts up to 547 nm from the native 482 nm [11], far short of the NIR target range of 700–900 nm. The D-luciferin-dependent luciferases from click beetle and firefly emit at satisfactory longer wavelengths, with emission maxima at 595 nm for the wild-type click beetle [12] and 616 nm for the engineered firefly luciferase [13,14]. In addition, D-luciferin analogues have been engineered to induce red [15] to NIR [16] bioluminescence without the need for luciferase manipulation. However, the ATP-requirement of the D-luciferin-dependent luciferases precludes their use in many *vivo* applications due to the extracellular ATP action as an inflammatory trigger of the immune response [17,18].

Consequently, alternative approaches have used Bioluminescence Resonance Energy Transfer (BRET). In BRET blue light photons from the luminescent *donor* undergo a non-radiative energy

* Corresponding authors. Address: Plate-Forme d'Imagerie Dynamique, Imagopole, Institut Pasteur, 25-28 Rue du Dr. Roux, 75724 Paris cedex 15, France (R. Tournebize).
E-mail addresses: regis.tournebize@pasteur.fr (R. Tournebize), spencer.shorte@pasteur.fr (S.L. Shorte).

1046-2023 © 2013 The Authors. Published by Elsevier Inc. Open access under CC BY-NC-SA license.
http://dx.doi.org/10.1016/j.ymeth.2013.09.005

transfer with spectrally suitable fluorescent *acceptor* molecules, thereby yielding an emission of red-shifted photons. Such resonance occurs under the strict condition where the juxtaposition of the respective molecular dipole moments is on the order of the Förster radius (2–13 nm, [19–21]), which is characteristic of the donor–acceptor pair. For example, the "far-red bioluminescent protein" (FBP), constructed by conjugation of an indocyanine dye to the *Cypridina* blue luciferase, exhibited an efficient red shift to 675 nm apparently due to BRET [22]. A plethora of other studies make claim to the same assertion that resonance is the underlying mechanism responsible for such luminescence red-shifting in the presence of suitable fluorophores ([23], and references therein). However, as a contrast to Fluorescence Resonance Energy Transfer, in which the donor displays a fluorescence lifetime change in the presence of the acceptor, the biochemical production of the BRET donor precludes the ability to synchronize donor production so as to measure such lifetime change and validate the mechanistic claims to resonance.

As an alternative mechanism entailing fluorophore-mediated red-shifting of bioluminescence, our recent studies have demonstrated the prevalence of the trivial radiative process under certain conditions [24]. This radiative phenomenon, or "Fluorescence by Unbound Excitation from Luminescence" (FUEL), has proved powerful since it bypasses the stringent need for a molecular proximity on the order of 10 nm. In our previous articles [24,25], red light was generated using an *Escherichia coli* strain expressing the *lux* operon (480 nm) in the presence of quantum dots, independently of covalent conjugation of the moieties. FUEL was empirically characterized both *in vitro* and *in vivo* as a method utilizing conventional epifluorescence phenomenon occurring between luminescent sources and spectrally compatible fluorophores. We demonstrated that FUEL occurs over mesoscopic distances from microns to millimeters under *in vivo* standard imaging conditions, which makes it highly exploitable in the context of macroscopic imaging (whole animal and blood samples). In this report, we establish that FUEL is a generally detectable phenomenon whose intensity dominates over resonance under certain *in vitro* conditions. Our results suggest how FUEL emerges as a promising new method for detection of molecular targeting and microscopic proximity at distances where Förster energy transfer vanishes.

2. Materials and methods

Bacterial strains and growth conditions. *E. coli* TOP10 (Life Technologies), *Klebsiella pneumoniae* 52145 [26] and *E. coli* DH5α (Life Technologies) constructs were grown in Luria Bertani (LB) broth at 30 °C supplemented with Ampicillin 100 μg mL^{-1}. *Photobacterium phosphoreum* ATCC 11004T was grown in LB supplemented with 0.5 M NaCl at 22 °C. Strains were grown aerobically on shakers at 250 rpm overnight.

Plasmids and reagents. 'pPpy_Green' designates the plasmid carrying the *Photinus pyralis* Green thermostable luciferase as a pGEX-6P-2 GST-fusion (pBR322 ori) [13] and 'pLux_Blue' the *Photorhabdus luminescens lux*ABCDE operon (colE1 ori) [27]. The Green *Renilla luciferase* expressing plasmid 'pGreen_Ren' was obtained as follows: the Targeting Systems (El Cajon, CA, USA) luciferase was PCR-amplified from pBasic-GrRenLuc using the primers 5′-ATGTCCGGCCTGAACGACATCTTCGAGGCTCAGAAAATCGAATGGCACGAA-ATGTTGTTGAAAGTTGTGTTTGCTATT-3′ and 5′-TGCCTG CTATTGCAGCACAGAA-3′, and ligated into the pTrcHis TA Expression cloning vector (Life Technologies). D-luciferin free acid (Interchim Cat # 27060I 1 × 1 g) was dissolved in 1X PBS (Ca- and Mg-free) and neutralized using KOH 3 M to a final pH of 7.4 to a final concentration of 30 mg mL^{-1}, and used as a substrate for pPpy_green-carrying constructs at a final concentration of 0.6 mg mL^{-1}. Coelenterazine *h* (Interchim, FW 407.5 g mol^{-1}) stock was dissolved in 1,2-propanediol to a concentration of 0.5 mg mL^{-1} and used as a 50× stock to a 25 μM final concentration. The rabbit polyclonal primary antibody (Ab) against formaldehyde-fixed *K. pneumoniae* 52145 cells, designated as 'α-Kp' (50 mg mL^{-1}), was generated in-house according to standard protocols. Fluorophores and Quantum dots were ordered from Life Technologies: Alexa-Fluor 647, 700 and 750 conjugates to streptavidin (Cat # S21374, S21383 and S21384) were dissolved in 400 μL 1× PBS to a final concentration of 139 μM fluorophore (DOS 3); Qtracker 705 non-targeted Quantum dots (Qd705, Cat #Q21061MP, Lot 1003186, 2.1 μM, QY 0.69); Qtracker 800 non-targeted Quantum dots (Qd800, Cat #Q21071MP, Lot 1081661, 2.0 μM, QY 0.49); Qd705 streptavidin conjugate (SA-Qd705, Cat #Q10161MP, Lot 1069891, 1.0 μM, QY 0.64).

Instruments. Luminescence and fluorescence measurements were acquired on a Perkin Elmer IVIS Spectrum or on a Monaco SAFAS Flx-Xenius XM as specified. Optical density (600 nm) and Bradford assay (595 nm) measurements were performed using a Beckman BioPhotometer. Plate absorbance at 500 nm (HABA assay) was done using the SAFAS.

Correction for time variation. Acquisition of the full luminescence spectra on the IVIS Spectrum necessitated correction for time variation of the signal over several minutes. Luminescence in the 520 nm filter, used as an arbitrary reference, was measured at regular intervals to infer the general trend of the signal. For each well, the 520 signal intensity was interpolated (cubic spline interpolation, Mathcad 2001 Professional) at the time of the measurement of other filters and used for the corresponding correction.

Biotinylation of the α-Kp antibodies. The primary antibodies were biotinylated using the Thermo Scientific Pierce EZ-Link Sulfo-NHS-LC-Biotin (Cat #21327) and the excess reagent was removed from the antibodies using the Thermo Scientific Pierce Zeba Spin Desalting Columns 7 K MWCO (Cat #89882). Protein concentration was measured using the standard Bradford assay (Haut du formulaire Bio-Rad reagent Cat #500-0006). The degree of biotinylation of the antibodies was measured using the Thermo Scientific Pierce HABA assay (Cat #28010). The α-Kp-biotA and α-Kp-biotB biotinylated antibody (Ab) batches were obtained by mixing 100 and 50 μL NHS reagent (10 mM, dissolved in 1× PBS) with 40 and 80 μL α-Kp antibody respectively, and displayed final degrees of substitution (DOS) of 16 and 4 biotin residues per Ab at final protein concentrations of 10 and 30 mg mL^{-1}.

Targeted FUEL. Four overnight replicate cultures of *K. pneumoniae* (pLux_blue), washed in 1× PBS, were resuspended in PBS to an OD of 4 (ca. 4×10^8 CFU mL^{-1} OD^{-1}). For each replicate, 100 μL PBS, α-Kp antibodies (2 μL α-Kp, 10 μL α-Kp-biotA, 10 μL α-Kp-biotB or 10 μL PBS for the control) and 100 μL cells were incubated 90 min at 30 °C. Cells were washed three times in PBS, and resuspended in 196 μL PBS. 4 μL of Qd705 or Alexa-647 streptavidin conjugate was added and incubated for 10 min at room temperature. Subsequently, 100 μL of the unwashed sample was loaded onto a 96-well plate, and 100 μL sample was washed twice in PBS, resuspended in 100 μL PBS and loaded onto a 96-well plate for measurements.

Luciferase expression, purification and assay. The thermostable *P. pyralis* green luciferase mutant (Ppy GR-TS in Branchini et al. [13]) was expressed and purified from *E. coli* TOP10 (pPpy_Green) according to the published protocol. The GST-tagged protein was eluted in 50 mM Tris–HCl (pH 7.5), 150 mM NaCl, 2% glycerol, 1 mM EDTA, 1 mM DTT and 10 mM reduced glutathione, and was stored at 4 °C supplemented with 800 mM ammonium sulfate (0.1 mg mL^{-1}). The enzyme (0.02 mg mL^{-1} final) was assayed in 50 mM Tris–HCl (pH 7.5), 10% glycerol, 1 mM DTT, 5 mM ATP, 5 mM $MgCl_2$ and D-luciferin 0.6 mg mL^{-1}.

3. Energy transfer mechanisms

Bioluminescence enzymatically produces a luminophore by converting the luciferase substrate into an exciton, which subsequently relaxes into the ground state product through emission of a photon. In the case of the firefly *P. pyralis* [14] or the click beetle *Pyrophorus plagiophthalamus* [12], the D-luciferin substrate is converted to excited oxyluciferin. The *Gaussia princeps* [28] and *Renilla reniformis* [29] convert coelenterazine to excited coelenteramide. Upon Fluorescence by Unbound Excitation from Luminescence (FUEL), the produced photons excite fluorophores at short-to-long distances (nm-cm) depending on the absorbance of the medium.

As a contrast, during Resonance Energy Transfer (RET) – or Förster energy transfer – the exciton energy is transferred non-radiatively to a neighboring fluorescent acceptor at distances on the order of the Förster radius R_0. At a donor–acceptor distance equal to R_0, which is typically 2–13 nm [19–21], this transfer is 50% efficient [21]. The distance R_0 (in nm), which is a characteristic of the donor–acceptor pair, depends on the donor quantum yield in the absence of the acceptor (Φ_D), the area-normalized donor emission spectrum $f_D(\lambda)$ and the acceptor absorbance spectrum – or molar extinction coefficient $\epsilon(\lambda)$ (M^{-1} cm^{-1}) [30]:

$$R_0^6 = \frac{900\Phi_D(ln10)\kappa^2}{128\pi^5 N_A n^4}\int_0^\infty f_D(\lambda)\epsilon(\lambda)\lambda^4 d\lambda \quad (1)$$

where N_A is Avogadro's number, λ the wavelength (in nm), n the refractive index of the medium (taken as 1.33 for water), κ^2 the orientation factor, taken as 2/3 for random donor–acceptor orientation.

For bioluminescence RET (BRET), the exciton quantum yield Φ_D can be measured from quantitative bioluminescence spectra (0.48 ± 0.07 for the firefly luciferase) [31] or from fluorescence quantum yield of the enzyme product [32] (0.47–0.51 for oxyluciferin [33]). Determination of the Förster radius R_0 allows for the estimation of the distance-dependent resonance energy transfer efficiency $E(r)$, where r is the donor–acceptor distance [34]:

$$E(r) = \frac{R_0^6}{R_0^6 + r^6} \quad (2)$$

From this expression, a mean exciton-fluorophore distance r_{DA} greater than $3R_0$ leads to a very low transfer efficiency ($\leqslant 0.01\%$), such that the exciton energy will be preferentially dissipated through a radiative process. For a variety of luminophore–fluorophore pairs of interest, R_0 was evaluated by taking the upper bound Φ_D value of 1 (Table 1):

Since the exciton is produced at the position of the enzyme, the occurrence of RET depends strongly on the exciton diffusion length L_D, which is the average distance the exciton can travel by diffusion over its lifetime [35]. L_D depends on the exciton diffusion coefficient D and lifetime τ as $L_D = (4D\tau)^{0.5}$ [36]. The exciton lifetime can be estimated from the fluorescence lifetime of the enzyme product [32,33], and is on the order of 4 ns for coelenteramide [37] and 2–10 ns for oxyluciferin depending on solvent polarity [33]. Small molecule diffusion coefficient in cells and aqueous environment is at most 10^{-5} cm^2 s^{-1} [38]. Calculating L_D from the values above yields a diffusion length upper estimate of 6.3 nm.

Dexter energy transfer via electron exchange, which is the other known non-radiative energy transfer mechanism [35], is only effective at distances shorter than for resonance (1–1.5 nm [39]). Hence, in the simple luminophore–fluorophore geometries of interest, the Dexter contribution can be neglected compared to RET [39]. Under conditions in which luminescence predominates over resonance, the resulting photons are free to excite fluorophores in the surrounding environment and produce red shifted photons via FUEL. Depending upon the experimental configurations, we discuss below the theoretical prevalence of luminescence over RET, and compare the theoretical RET contribution to the measured net increase in red photons upon fluorophore addition.

Table 1
Examples of Förster radii for luminophore–fluorophore pairs of interest.

	Alexa-647	Alexa-700	Alexa-750	Qd705	Qd800
Photobacterium	4.48	4.66	4.20	11.7	12.7
pLux_Blue	5.21	5.07	4.50	11.7	12.6
pGreen_Ren	5.80	5.40	4.73	11.6	12.27
pPpy_Green	6.26	5.67	4.93	11.5	11.9

4. FUEL in solutions

First, we will consider the case in which the luciferase and the fluorophore are unlinked and homogeneously distributed in solution. The luciferase can be packed in the bacterial cytoplasmic space, or mixed as purified enzyme. Due to the rapid kinetics of the exciton decay compared to its enzymatic formation [31], the exciton concentration is smaller than that of the luciferase enzyme. At concentrations of the fluorophore much higher than the purified enzyme or bacterial cells, the mean distances between fluorophores equals the mean distance between the fluorophore and the acceptor r_{DA}. The distance between molecules in solution can be estimated from c_f, the number of fluorophores per unit volume, using $r_{DA}^3 = 3/(4\pi c_f)$. Under the typical experimental conditions discussed below, the Alexa-Fluor concentrations are on the order of 4–14 μM, with a R_0 of 6.3 nm (Table 1), and the Quantum dots 40–180 nM with a R_0 of 12.7 nm. The corresponding RET efficiencies at the higher concentrations are 8×10^{-3}% and 9×10^{-5}% for the Alexa-Fluor and the Quantum dots respectively (Eq. (2)). Diffusion-enhanced energy transfer in solutions, discussed by Lakowicz [34], may become significant at the high diffusivity considered here (10^{-5} cm^2 s^{-1}), however, only for donor lifetimes greater than 100 ns. This is much greater than the fluorescence lifetimes for oxyluciferin and coelenteramide reported above (2–10 ns and 4 ns, respectively). Hence, we have shown that in the homogeneous unlinked configuration discussed below, the fraction of energy channeled through resonance is negligible compared to luminescence, and that diffusion-enhanced energy transfer effects can be neglected.

As an example of non-targeted FUEL, *E. coli* DH5α cells carrying the pLux_blue plasmid were mixed with non-functionalized Qd705 at the final concentration of 189 nM and visualized using a Perkin Elmer Ivis Spectrum CCD camera (Fig. 1). The filter signal was normalized to the Open filter of the PBS control. The 100 μL final volume was visualized in 96-well and 384-well plates, with respective depths of 2.14 and 8.15 mm. The increased well height afforded a greater increase of the red shifted photons compared to the PBS control (Fig. 1B). This mesoscopic geometric effect on the signal is not caused by resonance since the interspecies distance r_{DA} is conserved and is therefore a consequence of FUEL.

Such increase in red-shifted photons can be seen with a variety of luciferase-expressing bacterial suspensions and fluorophores (Fig. 2A–C), and seems fairly linear with increasing fluorophore concentrations (Fig. 2). The peak position of the red-shifted photons matches fairly well that of the corresponding fluorophore emission, with a peak at about 780 nm for the Alexa-Fluor750 (Fig. 2A), 800 nm for the Qd800 (Fig. 2B), and 680 nm for the Alexa-Fluor647 (Fig. 2D).

Addition of fluorophores to purified luciferase enzyme also displays FUEL (Fig. 3), with distinguishable fluorophore emission

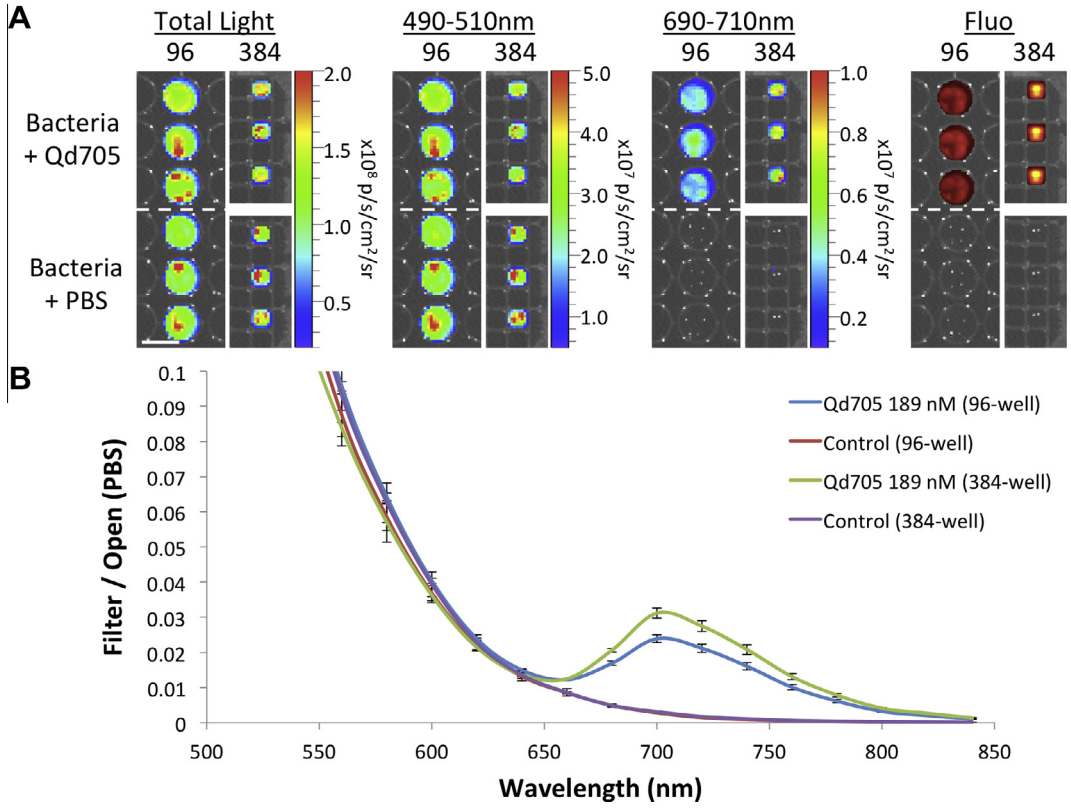

Fig. 1. Non-tageted FUEL with *E. coli* DH5a (pLux_Blue) mixed with Qd705. (A) Experimental setup and detection using the IVIS spectrum. (B) Resulting luminescence profile in 96- vs. 384-well plates with 189 nM Qd705.

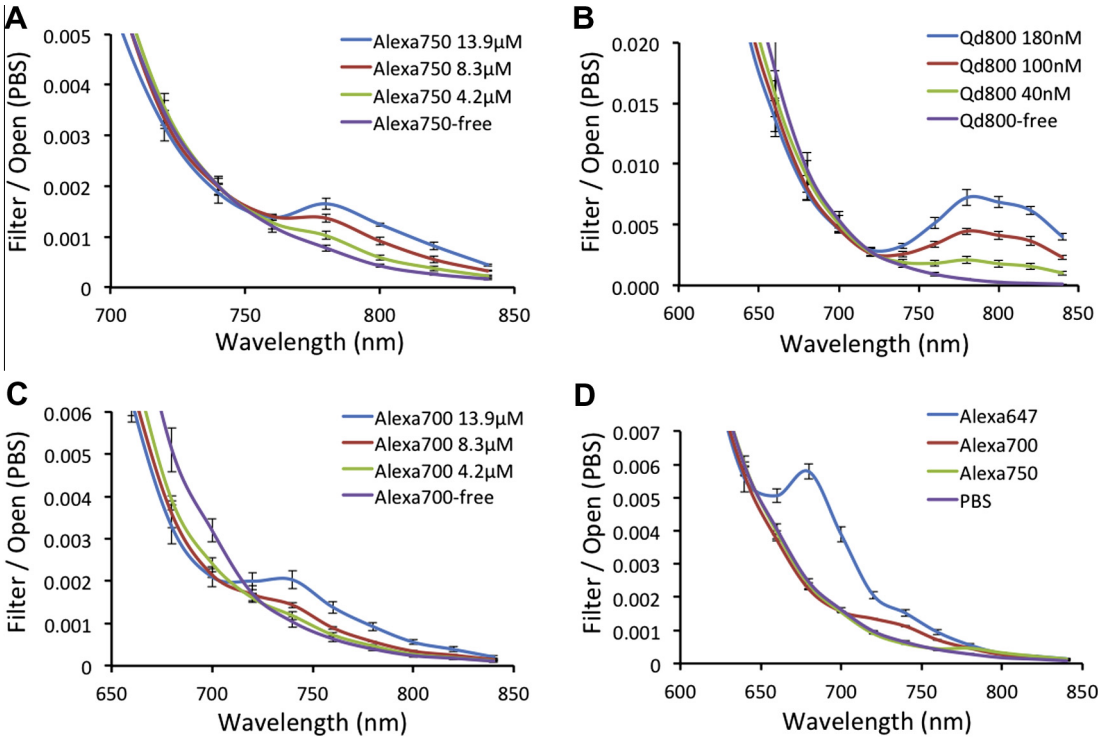

Fig. 2. Non-targeted FUEL between intracellularly produced luminophores and extracellular fluorophores. *E. coli* TOP10 (pPpy_Green) cells in 384-well plates, supplemented with D-luciferin substrate, and mixed with (A) SA-Alexa750 and (B) Qd705 at the indicated concentrations. (C) *E. coli* DH5α (pLux_Blue) in 384-well plates with SA-Alexa700 at the indicated concentrations. (D) *E. coli* TOP10 cells (pGreen_Ren) in 96-well plates with the indicated SA-Alexa fluorophore conjugates at 13.9 μM, supplemented with coelenterazine *h* substrate.

characteristic peaks as noted above. The lower photon-count observed in the red-to-near-infrared region compared to the PBS control, particularly significant in Figs. 2C and 3, may be caused by the absorption of the luminescence basal level by the Alexa-Fluor in that region. The large Stokes shifts for the Quantum dots compared to the Alexa-Fluors limit this effect with the former (Figs. 1 and 2B).

For homogeneously distributed fluorophores and excitons (or clusters of excitons as in a bacterial cell), the theoretical resonance contribution to the measured signal in various filters can be estimated using the RET efficiency expression $E(r)$ (Eq. (2)), which estimates the fraction of the total input signal (or Open filter signal) transferred by resonance at distance r. Importantly, akin to FUEL (or trivial radiative energy transfer), the total RET red-shifted photons distribute themselves according to the emission spectrum of the fluorophore. Hence in the 20 nm BP filters centered at a wavelength λ, the fraction of the RET photons $FF_{EM}(\lambda)$ emitted is:

$$FF_{EM}(\lambda) = \frac{\int_{\lambda-10}^{\lambda+10} F_{EM}(x)dx}{\int_0^{\infty} F_{EM}(x)dx} \quad (3)$$

where $F_{EM}(\lambda)$ is the fluorophore raw emission spectrum. As a first order approximation which accounts for the contribution of the nearest fluorophores, the net increase in photon flux $I_{RET}(\lambda, r_{DA})$ in the filter λ resulting from RET over a distance r_{DA} is:

$$I_{RET}(\lambda, r_{DA}) = I_{OPEN} \cdot FF_{EM}(\lambda) \cdot E(r_{DA}) \quad (4)$$

where I_{OPEN} is the photon flux ($p\ s^{-1}\ cm^{-2}$) in the open filter with no added fluorophore, which provides an estimate of the input flux of exciton energy which can be channeled though resonance. The distance r_{DA} can be estimated from the known fluorophore concentration as discussed above.

In order to ascertain the predominance of FUEL as the main energy transfer mechanism responsible for the increase of red-shifted photons upon fluorophore addition, the experimental values in Figs. 1–3 were compared to the theoretical RET contribution (Table 2). These results establish that resonance contributes at most 2.7% of the measured signal in the homogeneous setup described above. At the high concentrations used, RET may contribute a net increase in red photons on the order of 1% for the Alexa-Fluor and 0.001% for the Quantum dots.

5. Targeted FUEL

Second, we will consider the configuration in which fluorophores are targeted to the cell wall of bacteria expressing cytoplasmic luciferase (Fig. 4). The minimum distance between the cytoplasmic exciton and the extracellular fluorophore is the thickness of the cell wall, not accounting for targeting proteins such as antibodies (5 nm, [40]), streptavidin (5 nm, [41]) nor for the presence of a capsular layer (60–150 nm for *K. pneumoniae*, 10 nm for *E. coli* [42]). The bacterial cell wall thickness is typically greater than 30 nm [43]: in the Gram negative *E. coli*, the cell wall thickness reports vary between 30 nm [44] and 33 nm [45], while it is on the order of 40 nm in the Gram positive *Staphylococcus aureus* [45]. In addition, the analysis below neglects the physical characteristics of the commercial quantum dots, which commonly display a 8–11 nm-thick protective layer around the 4–8 nm diameter fluorescent core [46].

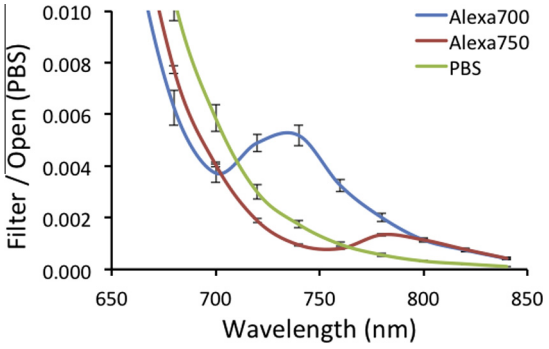

Fig. 3. Non-targeted FUEL using purified luciferase and fluorophores in solution. The *Photinus pyralis* green thermostable mutant protein (Branchini et al. [13]) was purified and assayed as described in Section 2, and visualized in 96-well plates upon fluorophore addition.

The excitons, which are generated uniformly within the cytosol, might diffuse significantly through the cell wall during their lifetime τ, allowing for the possibility of RET to occur. The exciton lifetime is the average duration between its production and its relaxation. The system geometry is described below using spherical coordinates, where r is the distance from the center of the bacterium, R_{cy} is the cytoplasmic radius of 500 nm, and R_F is the distance between the center of the bacterium and the targeted fluorophore (536 nm, Fig. 4B). The overall fraction of photons which undergo resonance (E_{tot}) can be calculated by multiplying the fraction of excitons at r by the RET efficiency $E(R_F - r)$, and integrating over r. The excitons are produced within the cytoplasm in which they are assumed to maintain a constant concentration. In addition, they diffuse through the cell wall during their lifetime τ of 10 ns to create a steady-state concentration gradient according to Fick's law of diffusion [36]. The contribution of the cytoplasmic excitons (E_{cyto}) is,

$$E_{cyto} = \frac{3}{R_F^3} \int_0^{R_{cy}} r^2 \cdot E(R_F - r)dr \quad (5)$$

and the contribution of the excitons diffusing through the cell wall (E_{cw}) is

$$E_{cw} = \frac{3}{R_F^3} \int_{R_{cy}}^{R_F} r^2 \cdot E(R_F - r) \cdot \mathrm{erfc}\left(\frac{r - R_{cy}}{\sqrt{4D\tau}}\right)dr \quad (6)$$

where the term erfc(x) denotes the complementary error function, and describes the steady-state exciton concentration gradient within the cell wall. For the calculations below, we chose the following more realistic parameters: a diffusion coefficient D of 5×10^{-6} cm^2 s^{-1}, which reflects the fact that diffusivity in cells is at least half that in water [38], an effective fluorophore-cytoplasm distance of 36 nm accounting for the size of the Ab–SA complex (Fig. 4B), and a lifetime τ of 10 ns. In the targeted configuration, the total RET contribution fraction for the Qdot, $R_0 = 12.6$ nm, is 1.2×10^{-4}, calculated according to Eqs.(5) and (6). For fluorophores the efficiency will be even lower as their Förster radius is usually much smaller. Hence, we have shown that in the targeted bacterial cell configuration described above, the fraction of energy channeled through resonance is negligible compared to luminescence, that is, a fraction on the order of 10^{-4} for the conservative parameters chosen.

As an example of targeted FUEL, *K. pneumoniae* bacterial cells were selectively labeled using biotinylated 1° antibodies, washed and added to a solution of streptavidin-conjugated Alexa-Fluor 647 or Qd705. This final solution was divided into an unwashed vs. a washed aliquot and tested for fluorescence and luminescence (Fig. 5). In order to provide an internal normalization factor analogously to BRET [47–50], the luminescence signal was normalized to the 500 nm filter signal (20 nm BP) for the Alexa-Fluor 647 and to the 600 nm signal for the Qd705. This normalization wavelength was chosen to exclude the region of fluorophore emission as well as minimize fluorophore absorbance. The use of such an internal control becomes important to resolve signal specificity when the

Table 2
Theoretical RET contribution to the measured net increase in red photons in homogeneous solutions.

Luciferase	Fluorophore[a]	Förster (nm)	Filter (nm)	Experimental I_{FILTER}/I_{OPEN}[b]	FF_{EM}	Theor. RET I_{RET}/I_{OPEN}	% RET/experimental
pPpy_Green	Alexa-750	4.93	780	8.72×10^{-4}	0.341	$5.96\ 10^{-6}$	0.68
pPpy_Green	Qd800	11.9	780	6.72×10^{-3}	0.341	$1.46\ 10^{-7}$	0.0022
pGreen_Ren	Alexa-647	5.8	680	3.33×10^{-3}	0.322	$1.51\ 10^{-5}$	0.45
pGreen_Ren	Alexa-700	5.4	740	4.79×10^{-4}	0.209	$6.36\ 10^{-6}$	1.3
pGreen_Ren	Alexa-750	4.73	780	1.76×10^{-4}	0.341	$4.70\ 10^{-6}$	2.7
Ppy enzyme	Alexa-700	5.67	740	3.45×10^{-3}	0.209	$8.53\ 10^{-6}$	0.25
Ppy enzyme	Alexa-750	4.93	780	7.79×10^{-4}	0.341	$5.99\ 10^{-6}$	0.77
pLux_Blue	Qd705	11.7	720	1.97×10^{-2}	0.486	$2.57\ 10^{-7}$	0.0013

[a] The Qdots are at a final concentration of 180 nM (130 nm approximate distance) and the Alexas at 13.9 μM (31 nm).
[b] Net increase in luminescence intensity in the specified filter upon fluorophore addition compared to the PBS control.

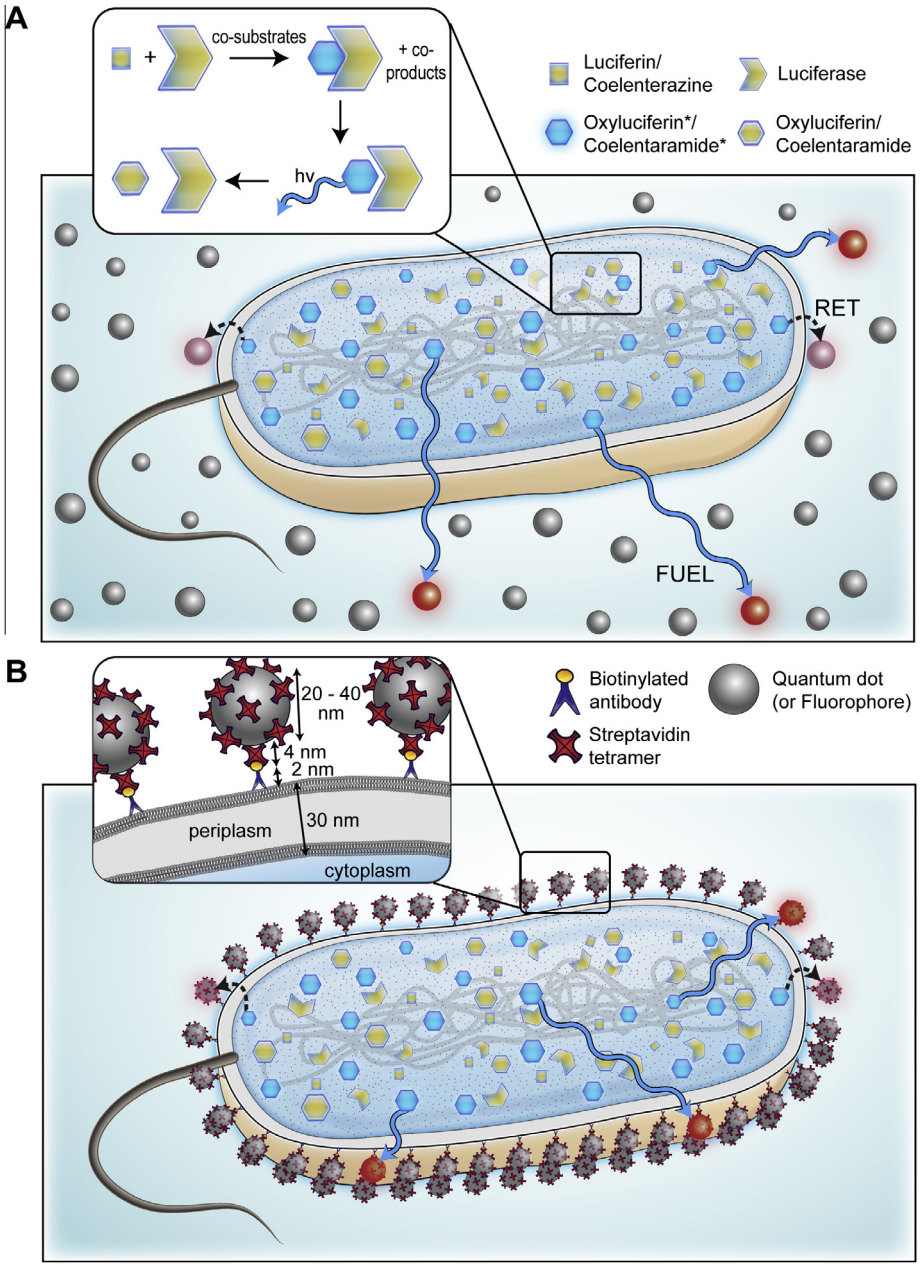

Fig. 4. Non-targeted (A) vs. targeted (B) FUEL using luciferase-expressing bacteria. (A) Inset: mechanistic representation of the exciton production by the luciferase. (B) Inset: example of targeting using biotinylated 1° antibodies recognizing the cell surface and streptavidin-conjugated Qdots. Illustration by Dr. A. Kawska at IlluScientia.com.

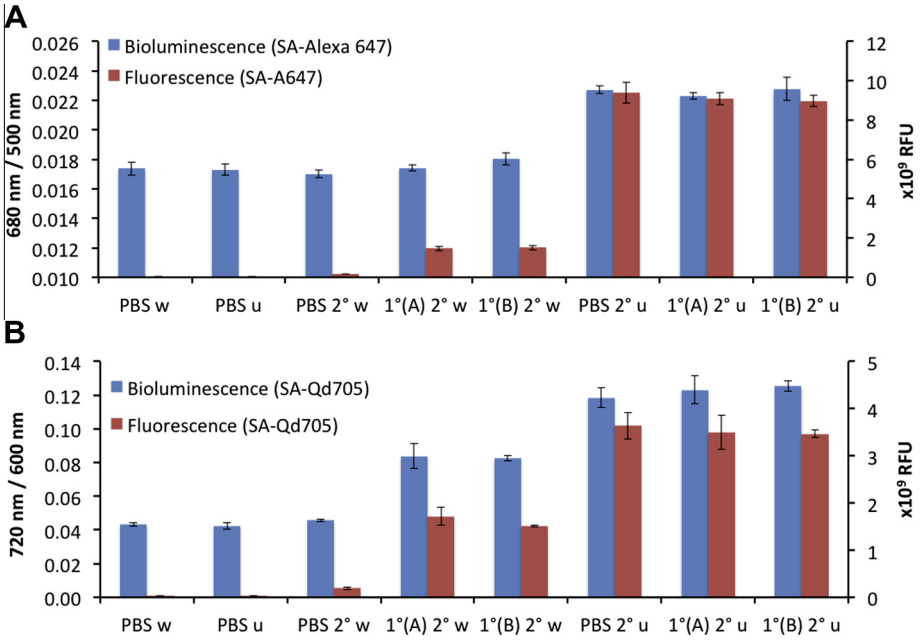

Fig. 5. Example of FUEL using *K. pneumoniae* (pLux_Blue) targeted with Alexa-647 or Qd705. K. *pneumoniae* was labeled with α-Kp-biotA antibody, noted 1° (A), α-Kp-biotB, noted 1°(B), or using PBS as a control. This was followed by the addition of a secondary component, noted as 2°: (A) SA-Alexa647 or (B) SA-Qd705, followed by a wash step 'w', or not 'u'. In the controls 'PBS w' and 'PBS u', PBS replaced the α-Kp Ab or the SA-conjugated fluorophore. The replicates are from four different overnight cultures.

various experimental steps affect the cells differently. For example, incubation of the cells with the primary antibody serum solution stimulated the luminescence compared to the PBS control (data not shown), which maybe due to nutrients present in the former.

In the case of the Alexa-Fluor 647 (Fig. 5A), the fluorescence levels indicate that about 16% of the added fluorophore was targeted to the cell surface at either degree of biotinylation, with about 10^6 fluorophores per cell. In the washed cells, this fraction of retained fluorophores does not lead to a significant increase in red-shifted photons compared to the basal luminescence level in the PBS controls. In other words, in the case of the Alexa-Fluor 647, the retained fraction of fluorophores after the wash is not able to elicit significant FUEL. In the unwashed cells, the Alexa-Fluor 647 addition leads to an indistinguishable increase in red photons in the targeted vs. untargeted cells. This result confirms that BRET is not taking place in this targeted configuration, since the reduced exciton/acceptor distance in the targeted configuration would lead to increased RET (Eq. (2)). In the case of the Qd705 (Fig. 5B) in the same configuration, 46% of the Qdots were retained by the cells (ca. 7000 Qdots per cell). This fraction was sufficient to lead to a significant increase in red signal in the washed cells. Nevertheless, in the unwashed Qdot samples, targeted and untargeted formations lead to the same increase in red signal. The net increase in red photons scales roughly linearly with the fluorophore concentration regardless of targeting, since the unwashed increase in red photons is about twice that of the targeted washed Qdots.

Therefore, despite the physical crowding of the fluorophores on the targeted bacterial surface, the photons generated within the cell respond solely to the bulk concentration of fluorophores. As a means to understand how this physical constriction does not translate into an optical constraint, the % optical coverage was calculated as the fluorophore absorption cross section σ (m^2) multiplied by the number of retained fluorophores divided by the surface area of the bacterium (assumed spherical, 1 μm diameter). An upper bound for σ (m^2) was calculated from the maximum extinction coefficient ϵ (M^{-1} cm^{-1}) as ϵ ln(10) 0.1 N_A^{-1}. The number of retained fluorophores were 335,000 and 6900 for the Alexa-Fluor 647 and Qd705, respectively, with ϵ on the order of 239,000 and 1.3×10^7 M^{-1} cm^{-1}, corresponding to maximum optical coverages on the order of 0.97% and 1.1%. This limited optical coverage accounts for the fact that the photons generated within the cells, despite targeting, are responding to the bulk concentration of the fluorophores in solution.The experimental net increase in red light upon fluorophore addition was compared to the theoretical RET contribution (Eqs. (5) and (6)) using the more realistic parameters estimates specified above. Under these conditions, RET contributes up to 4% of the measured increase in red light (Table 3).

These results indicate that FUEL can be used to resolve targeting in a homogeneous mix configuration but solely after a washing step (Fig. 5B). The washing step requirement to resolve targeting using FUEL inherently distinguishes this method from BRET, and further supports the theoretical calculations that BRET is not significant in the targeted case, and, therefore *a fortiori*, in the non-targeted case.

Table 3
Theoretical RET contribution to the measured net increase in red photons in the targeted configuration.

Fluorophore[a]	Förster[a] (nm)	Filter (nm)	Experimental I_{FILTER}/I_{OPEN}	FF_{EM}	Theor. RET E_{CYTO}[d]	Theor. RET E_{CW}[d]	% RET/experimental
Alexa-647	5.21	680	1.3×10^{-3},[b]	0.322	3.8×10^{-7}	2.1×10^{-7}	0.014
Qd705	11.7	720	1.4×10^{-3},[c]	0.486	7.7×10^{-5}	4.2×10^{-5}	4.0

[a] With the pLux_Blue as a donor.
[b] Net increase in the 680 filter in the unwashed Alexa-647 compared to the washed cells.
[c] Net increase in the 720 filter in the washed Qd705 cells compared to the PBS controls.
[d] For L_{CW} = 36 nm, R_{BACT} = 500 nm, τ = 10 ns and $D = 5 \times 10^{-6}$ cm^2 s^{-1}.

6. Perspectives

Our work presents FUEL as a conventional radiative excitation–emission process that is able to occur under experimental conditions where RET is negligible. In the mixed luminophore and targeted luminescent bacteria configurations, the minor resonance contribution was ascertained by comparing the intensity of the experimental signal to its theoretical resonance counterpart. Additional characteristics distinguish the behavior of the red-shifted FUEL photons from RET:

- The variation of the experimental red peak as a function of fluorophore concentration is quasi-linear, whereas in the case of resonance, a doubling in acceptor concentration would lead to a fourfold increase in red photons, due to the 6th power distance relation, which leads to a square concentration dependency.
- Depth, which is a macroscopic parameter, affects the experimental red peak intensity significantly at constant fluorophore concentration. In this case, the conserved microscopic distance between fluorophores does not affect intensity of the RET-dependent peak.
- Intensity of the red peak in the targeted-cell configuration is not significantly higher than in the untargeted control at constant fluorophore concentration, despite the decreased microscopic distance of a significant fraction of fluorophores upon targeting.

Significantly, while our results showed that FUEL can occur independently from RET, the converse cannot. FUEL is implicit as a second mechanism yielding red photons and is therefore an important, so far overlooked, component present in all RET measurements. For example, in the light of our work, Huang et al. [51] would likely interpret the slight red peak in the non-targeted RET controls as the FUEL contribution to the signal. This result [51] highlights the importance of designing appropriate RET controls to account for the non-specific FUEL contribution. The abundance of FUEL in any experimental condition will potentially alter the empirical interpretation of RET when it occurs. Arguably, given the minor RET contribution for quantum dots in solution shown in Table 1, the red peak observed by Zhang et al. [52] with luminol and non-targeted Qd800 at similar concentrations (200 nM) unlikely stems from resonance, all the more that the peak intensity does not follow the square dependency discussed above. Along with our results, other work [52] highlights the significance of FUEL as a means to enhance detection while alleviating the need for targeting. Consequently, the quantitative assessment of FUEL must be considered critical to the detection, quantification and interpretation of all fluorescence, bioluminescence and chemiluminescence RET-based studies under any conditions.

Acknowledgments

The authors would like to extend their gratitude for financial support from: Institut Carnot Pasteur *Maladies Infectieuses* (to A.D.H., J.D., A.R., R.T., S.L.S.); Pasteur Foundation of New York (to J.D.); *Region Ile de France* program DimMalInf (S.L.S., R.T.); Programme Inter Carnot Fraunhofer PICF 2011 *MEMI-OP* (F.R.); ANR Program *Grandes Investissement de l'avenir* Infrastructures Nationales en Biologie-Santé: *France LifebioImaging* (FLI) France Life Imaging (R.T., S.L.S.), *France Bioimaging* (J.D., S.L.S), Programme LabEx: Project *Biologie Intégrative des Maladies Infectieuses Emergentes* (IBEID); and Institut Pasteur, Paris. Further, the authors would like to thank Marie-Anne Nicola of the *Plate-Forme d'Imagerie Dynamique* for technical support and assistance; Cindy Fevre who generated the antibodies and Samantha Blazquez who purified them.

References

[1] K. O'Neill, S.K. Lyons, W.M. Gallagher, K.M. Curran, A.T. Byrne, J. Pathol. 220 (2010) 317–327.
[2] P.E. de Almeida, J.R.M. van Rappard, J.C. Wu, Am. J. Physiol. Heart Circ. Physiol. 301 (2011) H663–H671.
[3] M. Cronin, A.R. Akin, S.A. Collins, J. Meganck, J.-B. Kim, C.K. Baban, S.A. Joyce, G.M. van Dam, N. Zhang, D. van Sinderen, G.C. O'Sullivan, N. Kasahara, C.G. Gahan, K.P. Francis, M. Tangney, PLoS One 7 (2012) e30940.
[4] J.L. Miller, S. Murray, A.M. Vaughan, A. Harupa, B. Sack, M. Baldwin, I.N. Crispe, S.H.I. Kappe, PLoS One 8 (2013) e60820.
[5] T. Katsumata, H. Oishi, Y. Sekiguchi, H. Nagasaki, D. Daassi, P.-H. Tai, M. Ema, T. Kudo, S. Takahashi, PLoS One 8 (2013) e60411.
[6] D.K. Welsh, T. Noguchi, PLoS One 2012 (2012). pdb.top070607.
[7] Z. Shen, H. Röhr, K. Rurack, H. Uno, M. Spieles, B. Schulz, G. Reck, N. Ono, Eur. J. 10 (2004) 4853–4871.
[8] A. Miyawaki, D.M. Shcherbakova, V.V. Verkhusha, Curr. Opin. Struct. Biol. 22 (2012) 679–688.
[9] D.M. Shcherbakova, O.M. Subach, V.V. Verkhusha, Angew. Chem. Int. Ed. Engl. 51 (2012) 10724–10738.
[10] D.M. Shcherbakova, V.V. Verkhusha, Nat. Methods, advance online, publication (2013).
[11] A.M. Loening, A.M. Wu, S.S. Gambhir, Nat. Med. 4 (2007) 641–643.
[12] U. Stolz, S. Velez, K.V. Wood, M. Wood, J.L. Feder, Proc. Natl. Acad. Sci. USA 100 (2003) 14955–14959.
[13] B.R. Branchini, D.M. Ablamsky, M.H. Murtiashaw, L. Uzasci, H. Fraga, T.L. Southworth, Anal. Biochem. 361 (2007) 253–262.
[14] B.R. Branchini, T.L. Southworth, N.F. Khattak, E. Michelini, A. Roda, Anal. Biochem. 345 (2005) 140–148.
[15] N.R. Conley, A. Dragulescu-Andrasi, J. Rao, W.E. Moerner, Angew. Chem. Int. Ed. Engl. 51 (2012) 3350–3353.
[16] R. Kojima, H. Takakura, T. Ozawa, Y. Tada, T. Nagano, Y. Urano, Angew. Chem. Int. Ed. Engl. 52 (2013) 1175–1179.
[17] M. Idzko, H. Hammad, M. van Nimwegen, M. Kool, M.A.M. Willart, F. Muskens, H.C. Hoogsteden, W. Luttmann, D. Ferrari, F. Di Virgilio, J.C. Virchow, B.N. Lambrecht, Nat. Med. 13 (2007) 913–919.
[18] A. Trautmann, Sci. Signal. 2 (2009). pe6-.
[19] N. Hildebrandt, L.J. Charbonnière, H.-G. Löhmannsröben, J. Biomed. Biotechnol. 2007 (2007) 6.
[20] M. Kumar, D. Zhang, D. Broyles, S.K. Deo, Biosens. Bioelectron. 30 (2011) 133–139.
[21] P. Wu, L. Brand, Anal. Biochem. 218 (1994) 1–13.
[22] C. Wu, K. Mino, H. Akimoto, M. Kawabata, K. Nakamura, M. Ozaki, Y. Ohmiya, Proc. Natl. Acad. Sci. USA 106 (2009) 15599–15603.
[23] K.D.G. Pfleger, K.A. Eidne, Nat. Methods 3 (2006) 165–174.
[24] J. Dragavon, S. Blazquez, A. Rekiki, C. Samson, I. Theodorou, K.L. Rogers, R. Tournebize, S.L. Shorte, Proc. Natl. Acad. Sci. USA 109 (2012) 8890–8895.
[25] J. Dragavon, S. Blazquez, K.L. Rogers, C. Samson, R. Tournebize, S. Shorte, in: D.L. Farkas, D.V. Nicolau, R.C. Leif (Eds.), Proc. SPIE 7902, Imaging, Manipulation, and Analysis of Biomolecules, Cells, and Tissues IX, SPIE Digital Library, San Francisco, California, USA, 2011, pp. 790210–790210.
[26] X. Nassif, P.J. Sansonetti, Infect. Immun. 54 (1986) 603–608.
[27] K.-H. Choi, H.P. Schweizer, Nat. Protoc. 1 (2006) 153–161.
[28] T. Rathnayaka, M. Tawa, S. Sohya, M. Yohda, Y. Kuroda, Biophys. Acta – Protein Proteomics 1804 (2010) 1902–1907.
[29] W.W. Lorenz, R.O. McCann, M. Longiaru, M.J. Cormier, Proc. Natl. Acad. Sci. USA 88 (1991) 4438–4442.
[30] A. Bakayan, C.F. Vaquero, F. Picazo, J. Llopis, PLoS One 6 (2011) e19520.
[31] Y. Wang, H. Kubota, N. Yamada, T. Irie, H. Akiyama, Photochem. Photobiol. 87 (2011) 846–852.
[32] O.A. Gandelman, L.Y. Brovko, N.N. Ugarova, A.Y. Chikishev, A.P. Shkurimov, J. Photochem. Photobiol. B, Biol. 19 (1993) 187–191.
[33] P.E. Naumov, Y. Ozawa, K. Ohkubo, S. Fukuzumi, J. Am. Chem. Soc. 131 (2009) 11590–11605.
[34] J.R. Lakowicz, Principles of Fluorescence Spectroscopy, third ed., Kluwer Academic/Plenum Publishers, New York, 2006.
[35] A. Olaya-Castro, G.D. Scholes, Int. Rev. Phys. Chem. 30 (2011) 49–77.
[36] J. Welty, C.E. Wicks, G.L. Rorrer, R.E. Wilson, Fundamentals of Momentum, Heat and Mass Transfer, fourth ed., John Wiley & Sons Inc., New York, 2001.
[37] B. van Oort, E.V. Eremeeva, R.B.M. Koehorst, S.P. Laptenok, H. van Amerongen, W.J.H. van Berkel, N.P. Malikova, S.V. Markova, E.S. Vysotski, A.J.W.G. Visser, J. Lee, Biochemistry 48 (2009) 10486–10491.
[38] A.M. Mastro, A.D. Keith, J. Cell Biol. 99 (1984) 180s–187s.
[39] M.Y. Berezin, S. Achilefu, Chem. Rev. 110 (2010) 2641–2684.
[40] J.K. Armstrong, R.B. Wenby, H.J. Meiselman, T.C. Fisher, Biophys. J. 87 (2004) 4259–4270.
[41] F. Öisjöen, J.F. Schneiderman, A.P. Astalan, A. Kalabukhov, C. Johansson, D. Winkler, J. Phys. Conf. Ser. 200 (2010) 122006.
[42] Y. Meno, K. Amako, Infect. Immun. 58 (1990) 1421–1428.
[43] L.L. Graham, R. Harris, W. Villiger, T.J. Beveridge, J. Bacteriol. 173 (1991) 1623–1633.
[44] J.A. Hobot, E. Carlemalm, W. Villiger, E. Kellenberger, J. Bacteriol. 160 (1984) 143–152.
[45] J. Dubochet, A.W. McDowall, B. Menge, E.N. Schmid, K.G. Lickfeld, J. Bacteriol. 155 (1983) 381–390.

[46] I.L. Medintz, H.T. Uyeda, E.R. Goldman, H. Mattoussi, Nat. Mater. 4 (2005) 435–446.
[47] M.-K. So, C. Xu, A.M. Loening, S.S. Gambhir, J. Rao, Nat. Protoc. 24 (2006) 339–343.
[48] Y. Xu, D.W. Piston, C.H. Johnson, Proc. Natl. Acad. Sci. USA 96 (1999) 151–156.
[49] R. Arai, H. Nakagawa, A. Kitayama, H. Ueda, T. Nagamune, J. Biosci. Bioeng. 94 (2002) 362–364.
[50] S. Angers, A. Salahpour, E. Joly, S. Hilairet, D. Chelsky, M. Dennis, M. Bouvier, Proc. Natl. Acad. Sci. USA 97 (2000) 3684–3689.
[51] X. Huang, L. Li, H. Qian, C. Dong, J. Ren, Angew. Chem. 118 (2006) 5264–5267.
[52] N. Zhang, K.P. Francis, A. Prakash, D. Ansaldi, Nat. Med. 19 (2013) 500–505.